

# Excess Properties of Water-Methanol Mixtures as Studied by MD Simulations

G. Pálincás and I. Bakó

Central Research Institute for Chemistry of the Hungarian Academy of Sciences, Budapest

Z. Naturforsch. **46a**, 95–99 (1991); received November 12, 1990

*Dedicated to Dr. K. Heinzinger on the occasion of his 60th birthday*

Molecular dynamics simulations with pair interactions reproduce experimental excess properties of methanol-water mixtures. Water molecules lose, and methanol molecules gain neighbours in the mixtures as compared to the solvents. The water-methanol mixture with 0.25 mole fraction of methanol, resulting in extreme values for different excess properties, is characterized by the highest number of molecules with maximal number of H-bonded neighbours.

## Introduction

Water-alcohol mixtures show peculiar excess properties. Particularly, the excess heat of mixing  $\Delta H^E$  [1], excess partial molar volume  $\Delta V_2^E$  [2], excess molar heat capacity  $\Delta C^E$  [3], excess partial diffusion coefficients  $\Delta D_1^E$ ,  $\Delta D_2^E$  [4], excess adiabatic compressibility, UV absorption coefficient [5], and excess IR absorbance at the overtone region of spectra  $\Delta E^E$  [6, 7] have extreme values (mostly minima) approximately at the same alcohol concentrations. The point of maximal excess is typical for each alcohol and is near the methanol mole fraction  $x_m^* = 0.25$  for water-methanol mixtures.

The behaviour of the excess quantities in the concentration range  $0 \leq x_m \leq x_m^*$  is often interpreted as enhanced water-water interactions [8, 9] or an increase in the number of H-bonds in comparison to those present in the pure components. The concentration range around the transition point  $x_2^*$  (2 refers to the alcohol) is considered as a region of higher structural stability. The enhancement of the water structure is attributed to the formation of dense water structures in the hydration sphere of alcohol molecules which is associated both with the hydration of hydrophilic groups and clathrate structure formation around the hydrophobic groups of alcohol molecules. Contrary to the above conclusions, other authors ascribe the effect to the breaking of water structure [10, 11]. Structural changes as a result of increasing alcohol concen-

tration can be explained by the effect of hydrophobic interactions. The latter are assumed to take part only at low  $x_m$  values, whereas at higher concentrations, hydrogen bonding is thought to be influenced only by the interaction of water with polar groups of alcohol molecules [12].

In this work, the structural changes in water-methanol mixtures are studied by means of molecular dynamics (MD) simulation. MD simulations of pure solvents and two water-methanol mixtures,  $x_m = 0.1, 0.9$ , with flexible 3 site molecular models have been carried out recently [13–15]. To study the structure at the transition concentration, an additional MD simulation with 25 mol% methanol molecules has been carried out.

The results of five MD simulations with the same molecular models and interactions, two for pure solvents and three for mixtures will be discussed together. In the first paragraph a short description of the MD simulations is given. In the second paragraph the calculated excess properties are discussed, in the third we report structural evidences based on pair correlation functions, and in the forth paragraph we analyse the statistical got for H-bonding in mixtures.

A detailed discussion of the time dependent properties of the simulated mixtures is given elsewhere [16].

## I. MD Simulations

In the simulations the methanol and water molecules were represented by flexible three site models with force centers located on oxygen, hydrogen and methyl groups. The interaction potentials were repre-

Reprint requests to Dr. G. Pálincás, Central Research Institute for Chemistry, Hungarian Academy of Sciences, Budapest, Hungary.

0932-0784 / 91 / 0100-0095 \$ 01.30/0. – Please order a reprint rather than making your own copy.



Dieses Werk wurde im Jahr 2013 vom Verlag Zeitschrift für Naturforschung in Zusammenarbeit mit der Max-Planck-Gesellschaft zur Förderung der Wissenschaften e.V. digitalisiert und unter folgender Lizenz veröffentlicht: Creative Commons Namensnennung-Keine Bearbeitung 3.0 Deutschland Lizenz.

Zum 01.01.2015 ist eine Anpassung der Lizenzbedingungen (Entfall der Creative Commons Lizenzbedingung „Keine Bearbeitung“) beabsichtigt, um eine Nachnutzung auch im Rahmen zukünftiger wissenschaftlicher Nutzungsformen zu ermöglichen.

This work has been digitalized and published in 2013 by Verlag Zeitschrift für Naturforschung in cooperation with the Max Planck Society for the Advancement of Science under a Creative Commons Attribution-NoDerivs 3.0 Germany License.

On 01.01.2015 it is planned to change the License Conditions (the removal of the Creative Commons License condition “no derivative works”). This is to allow reuse in the area of future scientific usage.

sented by sums of intra- and intermolecular terms,

$$V_{\alpha\beta}(r, q) = V_{\alpha\beta}^{\text{intra}}(q) + V_{\alpha\beta}^{\text{inter}}(r),$$

where the  $q$  are internal coordinates and  $r$  distances between sites in different molecules. The intermolecular term in the total potential was separated into Coulombic and non-Coulombic contributions. Intramolecular parameters, bond lengths and angles for non-interacting monomers were represented by gas phase experimental values. The charges assigned to the sites together with the gas phase geometries result in dipole moments of 1.86 D for water and 1.93 D for methanol molecules. The form of the potentials and the potential constants used in simulations have been given elsewhere [13, 14].

The simulations were carried out at constant density and total energy. Ewald summation was used for all Coulomb interactions and the shifted force potential method for non-Coulombic contributions of site-site potentials. In all simulations the periodic cube contained 200 molecules. The following experimental densities were used:  $\rho_0 = 0.991 \text{ g cm}^3$ ,  $\rho_{0.1} = 0.9717 \text{ g cm}^3$ ,  $\rho_{0.25} = 0.9371 \text{ g cm}^3$ ,  $\rho_{0.9} = 0.8037 \text{ g cm}^3$  and  $\rho_1 = 0.7866 \text{ g cm}^3$ , where the index refers to the mole fraction of methanol molecules. Average temperatures for the different simulations were around 292 with deviations of about 6 K. The simulations were extended over 4–20 ps. The stability of the total energy was better than 0.1% during the entire length of the simulations, without rescaling the velocities.

## II. Interaction Energies and Heat Capacities

Total intermolecular energies ( $E_t$ ) of water-methanol mixtures together with potential energies of water ( $E_w$ ) and methanol molecules ( $E_m$ ) are compared with those for pure solvents in Table 1. The excess potential energies of mixing defined by

$$\Delta E = E_t - x_w E_w^0 - x_m E_m^0$$

(where  $E_w^0$  and  $E_m^0$  are the total intermolecular energies for pure solvents) are also compared in Table 1 with experimentally determined excess molar heats of mixing [1]. In this comparison the difference between enthalpy  $\Delta H$  and energy  $\Delta E$  can be neglected as  $p\Delta V$  is low compared to  $\Delta E$ . The data given in Table 1 show that the potential energy for water molecules is lower and that for methanol molecules is higher in the mixtures when compared with the pure solvents. This

Table 1. Total potential energies  $E_t$ , potential energies of water  $E_w$  and methanol  $E_m$  molecules and excess energies  $\Delta E$  and experimental excess molar enthalpies  $\Delta H$  in  $\text{kJ mol}^{-1}$ .

$x_m$	$-E_t$	$-E_w$	$-E_m$	$-\Delta E$	$-\Delta H(\text{exp})$
0	41.2	41.2	—	—	—
0.1	40.5	41.0	36.6	0.33	0.6
0.25	39.8	40.6	37.1	1.06	0.9
0.9	32.3	35.1	32.1	0.22	0.26
1.0	31.2	—	31.2	—	—

points to the destabilization of water molecules with increasing amounts of methanol molecules, and at the same time, the stabilization of methanol molecules in mixtures with increasing amounts of water molecules.

The calculated excess molar energies agree well with experimental excess molar heats of mixing and reproduce an extreme value for the mixture with 25 mole% methanol molecules.

It should be noted that for the calculation of the excess energies of mixing, the potential energies were taken from simulations with slightly different temperatures. However, the variation of the experimental  $\Delta H$  data is smaller than 0.1 kJ/mol per 10 K around room temperatures [1] and thus this should not much impair the comparison.

Constant-volume heat capacities ( $c_v$ ) have been calculated from the temperature fluctuations. In order to obtain measurable quantities we applied quantum corrections and corrections for the missing nine intermolecular modes of the  $\text{CH}_3$  group neglected in the 3-site methanol model [14]. In accordance with Berens et al. [17], quantum corrections were calculated in quantum harmonic oscillator approximation by treating the frequencies in the spectral densities as quantum oscillators. The uncorrected heat capacities, the corrections, and the excess molar heat capacities for the mixtures are given in Table 2. The quantum and methyl group corrections are proportional to the concentration of the components and therefore do not contribute to the excess heat capacities.

The obtained heat capacities for the pure solvents are by about 20% lower than the experimental ones. This seems to be a characteristic feature of the potential models applied. Unfortunately no experimental data are given in the literature. Interestingly, however, the calculated excess heat capacities are positive and show a minimum value for the mixture with  $x_m = 0.25$ , which resembles the properties of ethylalcohol-water mixtures [3].

Table 2. Constant volume heat capacities as calculated from temperature fluctuations  $c_v$ , quantum corrections  $\Delta c_v(q)$ , corrections for  $\text{CH}_3$  group  $\Delta c_v(\text{CH}_3)$ , corrected heat capacities and excess molar capacities in  $\text{J mol}^{-1} \text{K}^{-1}$ .

$x_m$	$c_v$	$\Delta c_v(q)$	$\Delta c_v(\text{CH}_3)$	$c_v(\text{corr.})$	$\Delta c_v$
0	97	−38.8	—	59	—
0.1	110	−37.0	1.0	74	16
0.25	93	−35.6	2.5	60	3
0.9	79	−28.4	9.0	60	7
1.0	69	−26.7	10.0	52	—

Table 3. Characteristic values of site-site pair correlations for mixtures and pure solvents ( $g(r_1)$  is the peak height at the first maximum at  $r_1$ ,  $n(r_m)$  is the coordination number integrated up to the first minimum  $r_m$ ). Distances are given in Å.

$x_m$	$\text{O}_w\text{--O}$		$\text{O}_m\text{--O}$		$\text{C--O}$	
	$g(r_1)$	$n(r_m)$	$g(r_1)$	$n(r_m)$	$g(r_1)$	$n(r_m)$
0	3.05	4.36	—	—	—	—
0.1	3.40	4.02	2.47	2.94	2.2	11.40
0.25	3.70	3.81	2.64	2.75	2.2	9.80
0.90	4.54	3.02	3.14	2.05	2.0	5.50
1.0	—	—	3.25	2.00	1.9	5.00

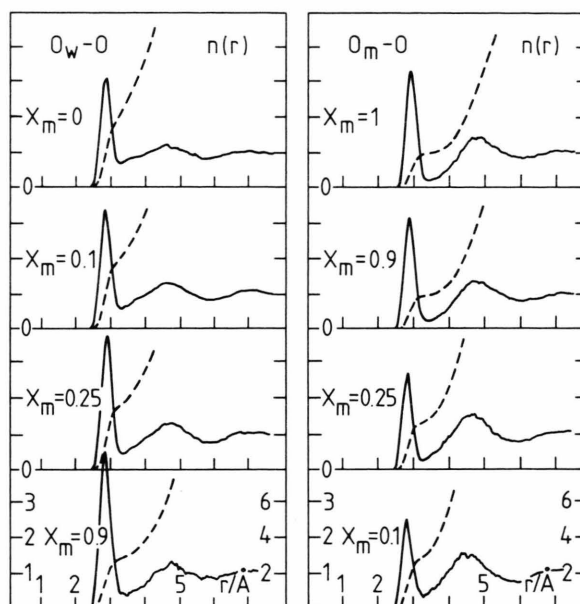


Fig. 1.  $\text{O}_w\text{--O}$  and  $\text{O}_m\text{--O}$  radial distribution functions and running integration numbers for pure water ( $x_m=0$ ), pure methanol ( $x_m=1$ ) and three water-methanol mixtures from MD simulations.

Considering the fact that the higher excess heat capacity is in accordance with the higher excess potential energy for water rich mixtures, it may be concluded that the major contribution to the excess heat capacities is due to configurational contributions. This may be attributed to the increasing stabilization of methanol molecules with increasing amounts of water molecules.

It has also been shown [16] that the self-diffusion coefficients for methanol and water molecules, obtained by MD, are smaller in the mixtures than in the pure solvents and, in agreement with experimental data, the lowest value for  $D_m$  is reached for the mixture with  $x_m=0.25$ . All three calculated data indicate a transition point for the 3:1 water-methanol mixture in accordance with the experimental results.

### III. Radial Distribution Functions (RDF)

For each mixture there are 15 different site-site RDFs  $g_{\alpha i \beta j}(r)$ , where  $\alpha, \beta = \text{O, H, C}$  and  $i, j = \text{m, w}$ . However, we use  $g_{\alpha i \beta}(r)$  RDFs in the present discussion. The first index,  $\alpha i$ , denotes  $\text{O}_w$ ,  $\text{O}_m$  and C sites, the second,  $\beta$ , stands for O and H foreign molecule H

sites, regardless whether they belong to water or methanol molecules. This representation is specially useful in characterizing differences between the extent of hydrogen bonding in mixtures and corresponding pure solvents.

The  $g_{\alpha i \beta}$  RDFs for mixtures together with those for the pure solvents are presented in Figs. 1–3. Some characteristic values of these RDFs are given in Table 3. The positions of the first intermolecular peaks in the  $\text{O}_w\text{--O}$  and  $\text{O}_m\text{--O}$  as well as in the  $\text{O}_w\text{--H}$  and  $\text{O}_m\text{--H}$  RDFs are the same within the limits of statistical uncertainty and found at  $2.84 \pm 0.002 \text{ Å}$  and  $1.9 \pm 0.02 \text{ Å}$ , respectively.

From the values given in Table 3 it can be seen that the  $\text{O}_w\text{--O}$  and  $\text{O}_w\text{--H}$  peak heights increase and the running coordination numbers integrated up to first minima ( $n(r_m)$ ) decrease with increasing molar ratio ( $x_m$ ) of methanol. The increase in the degree of correlation between water molecules and their nearest neighbours involves the loss of hydrogen bonded neighbours due to dilution with methanol molecules. In the methanol rich mixture ( $x_m=0.9$ ) there are in average only three oxygen and one hydrogen sites in the vicinity of water molecules. Compared with pure

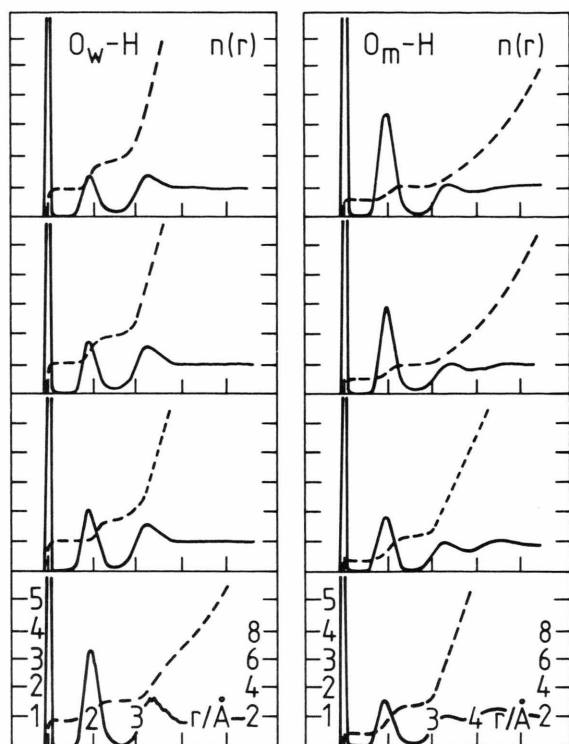


Fig. 2.  $O_w-H$  and  $O_m-H$  radial distribution functions and running integration numbers for pure water ( $x_m=0$ ), pure methanol ( $x_m=1$ ) and three water-methanol mixtures ( $x_m$ ) from MD simulations.

water this means the loss of one neighbour on the acceptor side.

Exactly opposite phenomena occur for the  $O_m-O$  and  $O_m-H$  RDFs of methanol molecules. The degree of correlation decreases and the number of H-bonded nearest neighbours increases with increasing concentration of water molecules in the mixtures. In the mixture richest in water ( $x_m=0.1$ ) a maximal number of H-bonded neighbours is reached, on average one on the donor, and two on the acceptor side of the methanol molecules.

The oxygen arrangement around the methyl groups is characterized for different mixtures in Fig. 3. The  $C-O$  nearest neighbour distance slightly decreases ( $0.1 \text{ \AA}$ ), the peak heights show a slight and the coordination numbers a remarkable increase with the increasing mole ratio of water molecules. More than twice as many neighbours are found near the methyl groups in the  $x_m=0.1$  mixture than in pure methanol. The hydrophobic effect observed in water-methanol mixtures is obviously due to packing reasons, simply because it is easier for water molecules to approach a

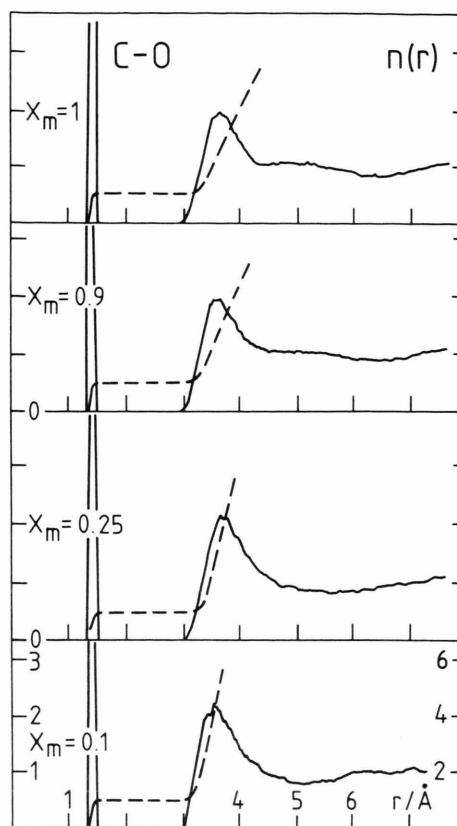


Fig. 3. Carbon-oxygen radial distribution functions and running integration numbers for pure methanol ( $x_m=1$ ) and three water-methanol mixtures ( $x_m$ ) from MD simulations.

methyl group than it is for methanol molecules with their bulky methyl groups.

#### IV. Hydrogen Bonding Analysis

There is no unambiguous definition of hydrogen bonds in MD simulations since all pair interactions change continuously as a function of separation and mutual orientation of the molecules. This can be seen both in the pair energy and hydrogen bond angle distributions ( $P(E)$ ,  $P(\vartheta_{HB})$ ) given in Figs. 4 and 5 for methanol and water molecules in mixtures and in pure solvents. Either the energetic or geometric concept is used for the definition of bonds; the choice of limiting values for variables is not given a priori. Therefore, both concepts classify bonds as strong and weak rather than bonded and broken. In the following, we use the geometric concept for the definition of H-bonds.

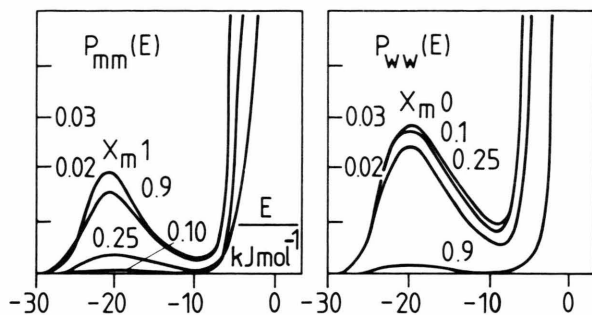


Fig. 4. Methanol-methanol and water-water pair energy distributions for pure solvent and different mixtures.

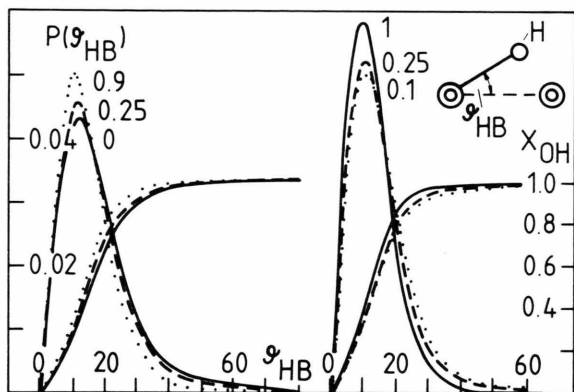


Fig. 5. Distribution of hydrogen bond angles  $\theta_{HB}$  and running bond angle integration number for water (left) and methanol (right) molecules.  $\theta_{HB}$  is defined in the insertion and  $x_m$  is indicated at the curves.

For comparison we consider two nearest neighbours, H-bonded on the condition that  $r_{O-O}$  is smaller than 3.4 Å (minimum in O–O RDFs) and the H-bond angle ( $\theta_{HB}$ ) defined in the insertion of Fig. 5 is lower than 20 degrees. It had been shown in a previous paper [14] that the above strong H-bond definition corresponds to an energetic one with limiting H-bond energy of about  $-10$  kJ/mol (minimum in the  $P(V)$  distribution in Fig. 4).

Table 4. Mean hydrogen bond angle  $\langle\theta_{HB}\rangle$ , mean number of hydrogen bonded neighbours  $\langle n_{HB}\rangle$ , mole fraction  $p$  of molecules having three,  $p_3$ , or four,  $p_4$ , hydrogen bonded neighbours, and mole fraction of H-bonded OH groups for methanol and water.

$x_m$	Methanol				Water			
	$\langle\theta_{HB}\rangle$	$\langle n_{HB}\rangle$	$p_3$	$x_{OH}$	$\langle\theta_{HB}\rangle$	$\langle n_{HB}\rangle$	$p_4$	$x_{OH}$
0	—	—	—	—	18.3	2.5	0.18	0.66
0.1	16.9	2.0	0.27	0.73	17.8	2.6	0.18	0.68
0.25	15.4	2.1	0.30	0.78	16.4	2.7	0.19	0.74
0.90	14.0	1.6	0.08	0.82	15.0	2.4	0.06	0.79
1.0	13.6	1.7	0.09	0.85	—	—	—	—

Some characteristic values for H-bonding of methanol and water molecules, such as the mean H-bond angle  $\langle\theta_{HB}\rangle$ , the average number of H-bonds per molecule  $\langle n_{HB}\rangle$ , and the mole fraction of molecules having a maximum number of H-bonds (3 for methanol and 4 for water) are given in Table 4.

It can be seen in Fig. 5 that no hydrogen bond angles higher than  $70^\circ$  exist between neighbouring molecules. The hydrogen bond angle distribution is narrower and the deviation from linearity of H-bonds is smaller for pure methanol than for pure water. The mean H-bond angle decreases for water and increases for methanol in the mixtures compared with the corresponding values of the pure solvents (Table 4). The number of methanol molecules with maximal number of H-bonds ( $P_3$ ) is higher in water rich mixtures. The highest number of molecules with maximal number of H-bonds is found for the water-methanol mixture with 25 mole% of methanol.

#### Acknowledgement

The authors are very grateful to K. Heinzinger for valuable discussions and critical remarks during the work. Financial support by Deutsche Forschungsgemeinschaft and the Hungarian Academy of Sciences is acknowledged.

- [1] S. Westmeier, Chem. Techn. Leipzig **28**, 350 (1976).
- [2] G. Onori, J. Chem. Phys. **87**, 1251 (1987).
- [3] L. A. K. Staveley, K. R. Hart, and W. I. Tupman, Discuss. Faraday Soc. **156**, 130 (1953).
- [4] W. Reinschussel and E. Hawlicka, Radiochemica Acta **31**, 157 (1982).
- [5] G. Onori, Nuovo Cim. **90**, 507 (1987).
- [6] G. Onori, Chem. Phys. Letter **154**, 212 (1989).
- [7] D. Bertoloni, M. Cassettari, and G. Salvetti, J. Phys. Chem. **78**, 365 (1983).
- [8] W. A. P. Luck, H. Borgholte, and T. Hatermehl, J. Mol. Struct. **177**, 523 (1988).
- [9] H. Enodo, Bull. Chem. Soc. Japan **46**, 1106 (1973).
- [10] H. Endo, Bull. Chem. Soc. Japan **46**, 1586 (1973).
- [11] R. Parshad, J. Acoust. Soc. Amer. **20**, 60 (1948).
- [12] G. H. Andrae, P. D. Edmons, and J. F. McKellar, Acustica **46**, 74 (1965).
- [13] G. Jancsó, P. Bopp, and K. Heinzinger, Chem. Phys. **85**, 377 (1984).
- [14] G. Pálincás, E. Hawlicka, and K. Heinzinger, J. Phys. Chem. **91**, 4334 (1987).
- [15] G. Pálincás, E. Hawlicka, and K. Heinzinger, 1990 submitted.
- [16] G. Pálincás, I. Bakó, K. Heinzinger, and P. Bopp, 1990 submitted.
- [17] P. H. Behrens, H. J. Mackay, G. M. White, and K. R. Wilson, J. Chem. Phys. **79**, 2375 (1983).